Electronic Supplementary Information

Controllable Ag nanoparticles coated ZnO nanorod arrays on alloy substrate with enhanced field emission performances

Mengjie Li, Weijun Huang, Weijin Qian,* Boyang, Liu, Hao Lin, Wei Li, Li Wan, and Changkun Dong*

Institute of Micro-nano Structures & Optoelectronics, Wenzhou University, Chashan University Town, Wenzhou, Zhejiang 325035, China

E-mail: weijinqian@wzu.edu.cn and dck@wzu.edu.cn

Index

SI-1 Comments on the random and well aligned ZnO NRs arrays

As reported in the literatures, proper thickness and good homogeneity of nucleation layer, as well as the heteroepitaxy or homoepitaxy substrates may be beneficial for the growth of aligned ZnO nanorods.[1-3] In our experiment, the ZnO seed solution was coated on the substrates by spin-coating method, so it is difficult to control the homogeneity of nucleation layer (ZnO seed layer). In addition, the alloy substrate cannot be strictly regarded as a homoepitaxy substrate due to some rough areas on the surface.

Field emission (FE) properties of a material depend mainly on its work function and field enhancement factor as described by the Fowler–Nordheim (FN) theory.[4] The field enhancement factor is related to the morphologies, e.g. aspect ratio[5] and density,[6] of the field emitters. Comparing with the random ZnO NRs arrays, well aligned ZnO NRs arrays may have larger growth density and it will lead to the higher screening effect, which might not benefit the improvement of the FE properties.

SI-2 TEM image of the Ag-ZnO-20 product

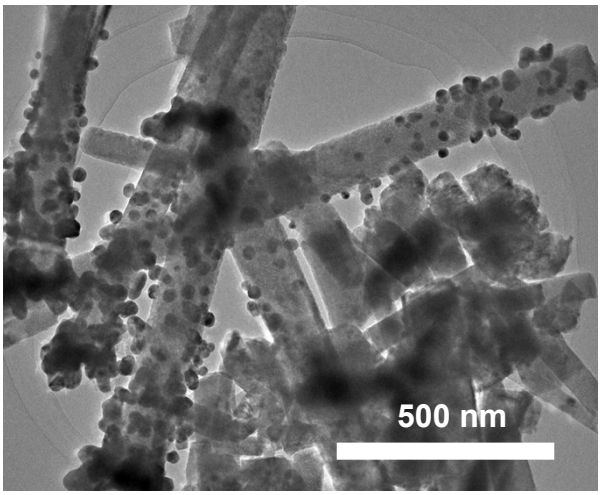

Fig. S1 TEM images of the Ag-ZnO-20 product

To better observe morphology of the product, TEM image of the Ag-ZnO-20 composite is shown in Fig.S1. As shown in Fig.S1, ZnO nanorods have the diameters of about 120 nm and they are coated with some Ag nanoparticles with the diameters of 5-25 nm.

SI-3 XRD pattern of the products

As shown in Fig. S2, XRD characterization suggests that the three peaks at 31.8^{o}, 34.4^{o} and 36.3^{o} are from the (100), (002) and (101) planes of ZnO nanorods,[7,8] respectively. In addition, the intensity of the (002) peak is much higher than the other two peaks, suggesting

that the ZnO nanorods is highly grown along the c-axis orientation. The other two peaks could be from (111) and (220) crystallographic planes of Ni, which came from the alloy substrate.[9] In comparison with the pristine ZnO nanorods, the peak of metal Ag (111) appeared at 38.2° in the Ag-ZnO-20 sample.[10]

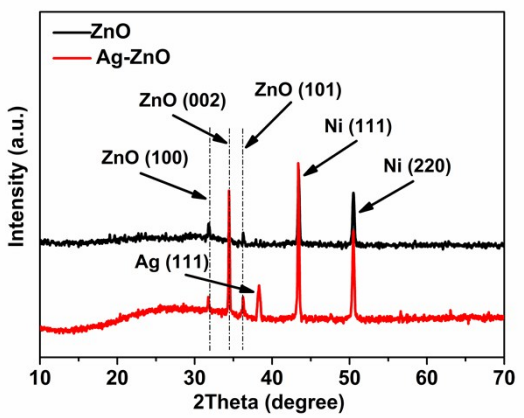

Fig. S2 XRD pattern of the pristine ZnO nanorods and Ag-ZnO-20 composite.

SI-4 EDS mapping of the Ag-ZnO-20 product

EDS mapping of the Ag-ZnO-20 product are shown in Fig.S3. The components of the Ag-ZnO product exhibit the signals of Zn, O, and Ag, as expected. In addition, Zn and O elements are better distributed than that of Ag element.

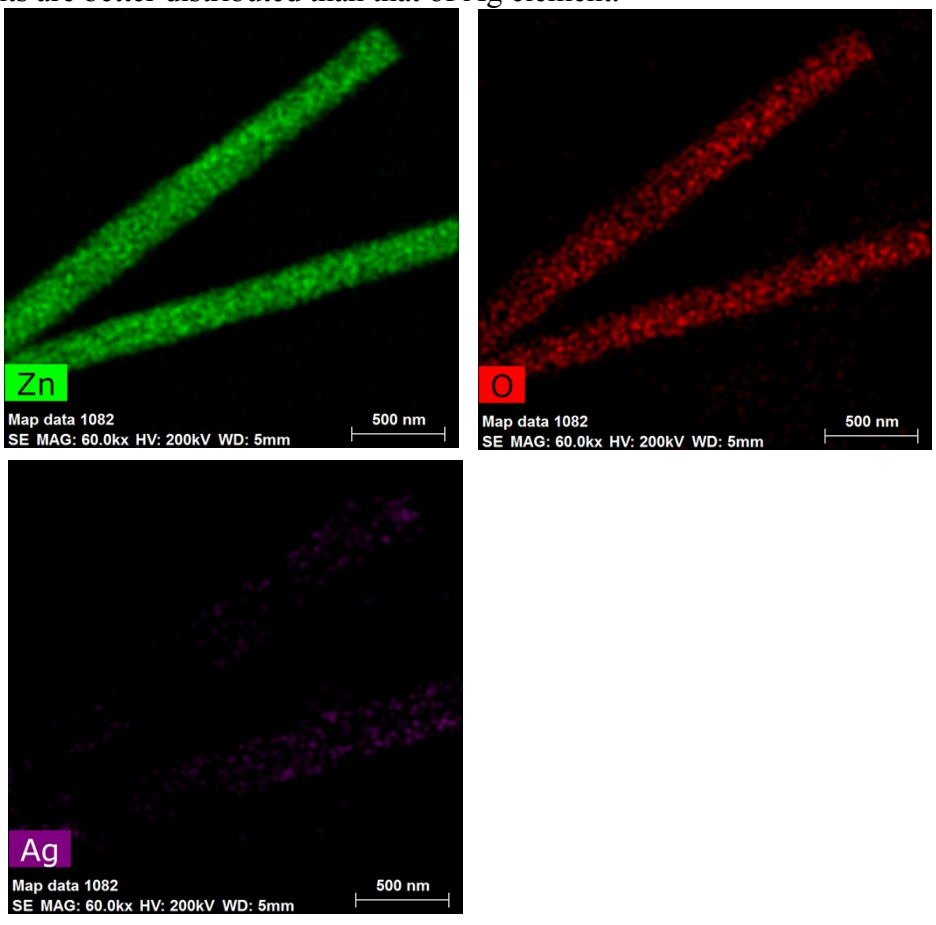

Fig. S3 EDS mapping of the Ag-ZnO-20 product

SI-5 XPS data on the elemental contents of the Ag-ZnO-20 sample

Table S1 XPS data on the elemental contents of the Ag-ZnO-20 composite

Sample	C (%)	O (%)	Zn (%)	Ag (%)
Ag-ZnO-20	50.48	26.55	14.4	8.57

Actually, the ZnO prepared by the hydrothermal method is not stoichiometric, as reported in the literatures.[11,12] Because different defects in the ZnO nanorods, such as Zn interstitials or oxygen vacancies, are formed during the hydrothermal reaction, due to the high Zn concentration and low oxygen concentration in the reaction solution.[11] In addition, according to the O1s spectrum (See Fig.4c in the Main Text), the O signals are from ZnO, defect O and adsorption O. From the integral intensity of the three deconvolution peaks, it is estimated that O contributions from ZnO, defect O and adsorption O are 0.315, 0.600 and 0.085, respectively. Due to the total O contribution of 26.55%(see Table S1), O contribution from ZnO is estimated to be about 8.36%,while Zn from ZnO is 14.4% (see Table S1).

SI-6 Explanation of the attribution for C peak

Because the Ag-ZnO sample was prepared by two methods, i.e. synthesis of ZnO nanorod arrays (ZNAs) by a hydrothermal method, followed by electrophoretic deposition method to coat ZNAs with the Ag nanoparticles. Actually, the product prepared by these methods did not show the existence of the carbon species, as reported in literatures.[9,13,14] In addition, EDS result of Ag-ZnO sample did not show obvious C signal (see Fig.3d in the Main Text).Therefore, we believe that the C peak comes from the sample holder in the XPS chamber.

SI-7 Explanation of the deconvolution peaks: oxygen defect and the chemisorbed oxygen from O1s

As for the oxygen defect, because different defects in the ZnO nanorods, such as oxygen vacancies, are easily formed during the hydrothermal reaction, due to the high Zn concentration and low oxygen concentration in the reaction solution.[11,12]As for the chemisorbed oxygen, according to the previous reports,[15,16] the high-energy peak was from the surface oxidation when exposing ZnO films to the air. In our experiments, the samples were conducted the annealing process, which might experience a surface oxidation process due to the presence of small amounts of oxygen.

SI-8 Work function measurement of the Ag-ZnO-20 sample

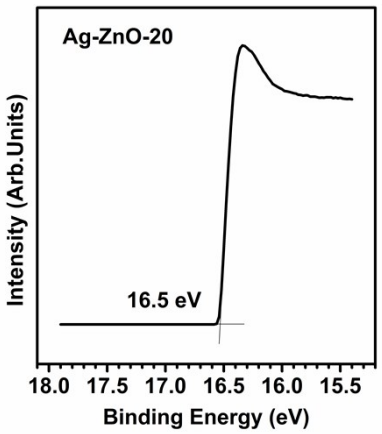

Fig. S4 The binding energy of the secondary electron cutoff edge.

The Valance band (VB) spectra were measured with a monochromatic He I light source (21.2eV) and a VG Scienta R4000 analyzer. A sample bias of −5 V was applied to observe the secondary electron cutoff. The work function (ϕ) can be determined by the difference between the photon energy and the binding energy of the secondary cutoff edge. The work function（ϕ) of Ag-ZnO-20 sample is measured to be about 4.7 eV（21.2-16.5=4.7 eV).

References

1. Y. Tak and K.Yong, J. Phys. Chem. B, 2005, 109, 19263-19269

2. L. E. Greene, M. Law, D. H. Tan, M. Montano, J. Goldberger, G. Somorjai, and P. D. Yang, Nano Lett., 2005, 5, 1231-1236.

3. Z. Liu, J. Ya, E. Lei, J. Solid State Electr., 2010, 14, 957–963.

4. W. J. Qian , H. W. Lai , X. Z. Pei , J. Jiang , Q. Wu , Y. L. Zhang , X. Z. Wang and Z. Hu, J. Mater. Chem., 2012, 22, 18578-18582.

5. Z. Xu, X. D. Bai and E. G. Wang, Appl. Phys. Lett., 2006, 88, 133107.

6. N. Liu, Q. Wu, C. Y. He, H. S. Tao, X. Z. Wang, W. Lei and Z. Hu, ACS Appl. Mater. Interfaces, 2009, 1, 1927–1930.

7. Z. J. Gu, M. P. Paranthaman, J. Xu, and Z. W. Pan, ACS Nano, 2009, 3, 273–278.

8. S. Cho, S. Kim, N. H. Kim, U. J. Lee, S. H. Jung, E. Oh, and K. H. Lee, J. Phys. Chem. C, 2008, 112, 17760-17763.

9. J. P. Liu, X. T. Huang, Y. Y. Li, X. X. Ji, Z. K. Li, X. He and F. L. Sun, J. Phys. Chem. C, 2007, 111, 4990–4997.

10. S. S. Warule, N. S. Chaudhari, R. T. Khare, J. D. Ambekar, B. B. Kale and M. A. More, CrystEngComm, 2013, 15, 7475–7483.

11. J. P. Liu, C. X. Xu, G. P. Zhu, X. Li, Y. P. Cui, Y. Yang and X. W .Sun, J. Phys. D: Appl. Phys., 2007, 40, 1906–1909.
12. Y. Sun, D. J. Riley, and M. N. R. Ashfold, J. Phys. Chem. B 2006, 110, 15186-15192.
13. S. Xu, C. S. Lao, B.Weintraub, and Z. L. Wang, J. Mater. Res., 2008, 23, 2072-2077.
14. J. J. Qiu, X. M. Li, W. Z. He, S. J. Park, H. K. Kim, Y. H. Hwang, J. H. Lee and Y. D. Kim, Nanotechnology, 2009, 20, 155603.
15. L.W. Lai, C. T. Lee, Mater. Chem. Phys., 2008,110, 393-396.
16. S. Major, S. Kumar, M. Bhatnagar, K. L. Chopra, Appl. Phys. Lett., 1986, 40, 394.